COMPARISONS OF PRD COMPONENTS FOR VARIOUS EBR-II CONFIGURATIONS

by

D. Meneghetti and D. A. Kucera

Argonne National Laboratory
Argonne, Illinois
60439-4820

Submitted for the

ANS Topical Meeting on Advances

in Reactor Physics and Safety

September 17-19, 1986

Saratoga Springs, New York

DISCLAIMER

Comparisons of PRD Components for Various EBR-II Configurations*

D. Meneghetti and D. A. Kucera

Argonne National Laboratory
Argonne, Illinois

ABSTRACT

Comparison of detailed calculations of contributions by region and component of the power-reactivity-decrements (PRD) for four differing loading configurations of the Experimental Breeder Reactor-II (EBR-II) are given. The linear components and Doppler components are calculated. The non-linear (primarily subassembly bowing) components are deduced by differences relative to measured total PRD values. Variations in linear components range from about 10% to as much as about 100% depending upon the component. The deduced non-linear components differ both in magnitude and sign as functions of reactor power. Effects of differing assumptions of the nature of the fuel-to-clad interactions upon the PRD components are also calculated.

1. INTRODUCTION

The operation and use of the Experimental Breeder Reactor II (EBR-II) as a fast-reactor facility for the irradiation of test fuels, structural materials, and absorbers and for operational-transient studies have led to the need for improved understanding of feedback characteristics [1]. The EBRPOCO computer program [2] together with a program addition (RODCO), which accounts for effects of axial positionings of the control rods, are specifically designed to facilitate the calculation of the detailed linear components and Doppler components of the power reactivity decrement (PRD). Furthermore, the sums of these contributions subtracted from the corresponding measured PRD values enable the nonlinear (subassembly-bowing) component to be deduced. Because the loading configurations are heterogeneous and frequently modified, knowledge of the dependencies of the various components on the configuration is important for interpretation of steady-state and operational-transient results.

The linear components of the PRD for EBR-II runs 85A, 93A, 99A, and 122A have been calculated and compared. These runs were chosen for this study because they represent a range of differing loading patterns and/or of differing measured total PRD values. To minimize effects of uncertainties in absolute values of measured primary flows, these four loadings were also chosen because they had identical measured total flows. Inter-comparisons of the calculated results and of the deduced nonlinear components obtained by comparisons with the measured PRDs are then less affected by the accuracy of the absolute total-flow measurement. (In these studies the calculated reactivities in units of $\%\Delta k/k$ were converted to inhour units by the factor 441 Ih per $\%\Delta k/k$. Measured reactivities were in inhours or cents. If in cents conversion to inhour units was made by the factor 3 Ih per ¢ corresponding to $\beta_{eff} \cong 0.0068$.)

*Work supported by the U. S. Department of Energy, Reactor System, Development and Technology, under Contract W-31-109-Eng-38.

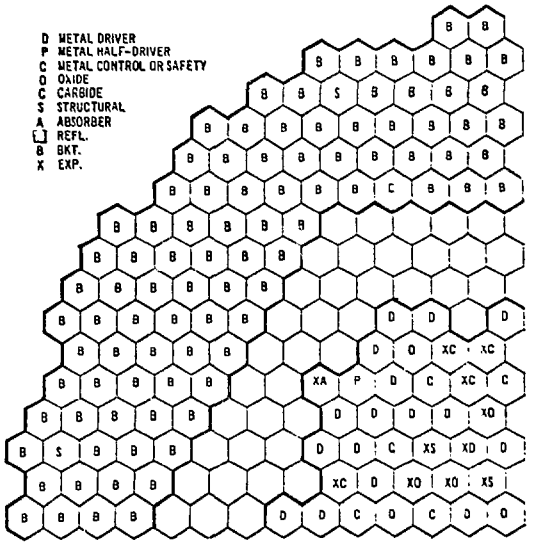

One quadrant of the EBR-II run 99A loading pattern is shown in Figure 1. The subassemblies in the central region constitute the core, where letter X denotes experimental subassemblies of the indicated types. The surrounding unlettered subassemblies are the steel radial-reflector subassemblies. The subassemblies of the outer region designated by letter B comprise the metallic depleted-uranium radial blanket. The accompanying legend in Figure 1 enables the subassembly types to be identified. The subassembly-cell areas are about 30 square centimeters. The axial height of the core region is about 34.5 centimeters and the overall axial dimension including lower and upper axial reflectors is about 135 centimeters.

Figure 1. One Quadrant of Run 99A

2. EBRPOCO INPUT

Intra-subassembly information required as direct input for EBRPOCO consists of element and rod diameters, number of fueled elements, type of fuel, fuel diameter, clad thickness, gap status, number of structural rods which are solid, and number of structural rods designated as non-solid (containing test samples or experiments). The fuel types are designated as metal driver, mixed-oxide, mixed-carbide, and uranium-metal blanket. The gap status is either open or closed. An open gap is specified to contain sodium or helium and if helium-bonded contains xenon tag gas. A closed gap is specified as having fuel expanding axially either freely or as determined by the axial expansion of the cladding.

By the nature of the input data it requires, EBRPOCO is the final step of a computational process involving also prior executions of other programs. Three-dimensional subassembly-wise non-gamma and gamma energy deposition rates are required. These are obtained from XY-geometry neutron and gamma calculations in which every subassembly is represented as a rectangle having four mesh regions. From corresponding azimuthally-homogenized RZ-geometry analyses are obtained non-gamma and gamma axial distributions of the energy deposition rates. These are 30 energy group discrete-ordinate neutronics calculations in S_4 transport approximation and 20 energy group gamma calculations in P_3S_4 approximation using an EBR-II modification of the DOT [3] program. The composite of the results from the two geometries is used to model the required three-dimensional input and to obtain overall power normalization. This synthesis is carried out using an auxiliary EBR-II program.

Required EBRPOCO inputs are also the subassembly-homogenized compositions (used in the XY-geometry calculations) and the regional compositions and axial delineations (used in the RZ-geometry calculations). The calculated spatial distribution of gamma energy deposition rate per unit mass of steel is also required. The latter input is needed for the EBRPOCO calculation of the gamma energy deposition rates in steel materials of a subassembly, for example, structural rods, hexagonal cans,

etc. The sum of these deposition rates is also subtracted from the total gamma energy deposition rate for a given axial interval of a subassembly. The remaining gamma energy deposition rate is then added to the non-gamma deposition rate and the sum attributed to the fuel-containing elements of the subassembly.

The program also required the spatial distributions of isotopic reactivity-worths. These are currently obtained from RZ-geometry calculations using the perturbation theory option of the CITATION [4] program. For computation of the distributions of the Doppler component a higher temperature neutron cross section set is needed. Subassembly coolant-flow is obtained from calculations carried out using the EBRFLOW [5] program.

3. LINEAR COMPONENTS

For each core, steel-radial-reflector, or depleted-uranium radial-blanket subassembly of an EBR-II loading configuration, the subassembly area-averaged axial distributions of the temperatures of sodium coolant, fuel- and blanket-element claddings, structural rods and steel reflectors, sodium in gaps, and fuel were calculated. Axial distributions of the components of the PRD for the subassemblies were then obtained for the components resulting from: coolant density (density reduction of sodium coolant due to temperature), coolant displacement (displacement of sodium coolant by thermal radial expansion of cladding, structural rods, subassembly cans, and lower and upper axial-reflector regions), steel density (density reduction of these steel components due to axial expansion with temperature), bond sodium (resultant of displacement of bond sodium, if present in the open gaps, by differential thermal expansions of fuel and cladding and of density reduction of bond sodium due to temperature), fuel and blanket axial expansions (free axial expansion of fuel if unrestricted by cladding or restricted axial expansion of fuel determined by axial expansion of cladding), Doppler (in fuel and blanket), B_4C-fuel (change in separation of B_4C follower and fuel in the cases of high-worth fueled control rods having B_4C followers), and the rod bank suspension (downward expansion of the control rods because of their being suspended from above). For the rod bank suspension EBRPOCO calculates the downward expansion of each rod from its banked position. The contributions of the rods to the bank suspension component of the PRD are then obtained by using the measured rod worths together with the measured fractional differential worth curves for the rod types.

Because EBRPOCO was specifically developed for EBR-II loadings the thermal conductivity and thermal expansion functions for the metal driver fuel and the mixed-oxide and mixed-carbide fuels irradiated in EBR-II are internally programmed. Furthermore, because EBR-II loadings contain fuels with various burnups, as well as differing fuel types, the type of fuel-cladding interaction assumed for a subassembly was based upon the type of fuel and the estimated average fuel burnup of the subassembly. Thus the fueled subassemblies are assumed to have gaps either: fully open, fully closed with fuel free to move axially, or fully closed with fuel axially restrained by the cladding. For Mark II fuel, in the latter case, it was also assumed that about one-third of the fuel porosity contained sodium.

Regional results for these processes for runs 85A, 93A, 99A, and 122A are given in Tables I to IV, respectively. The PRD calculational results are for an assumed power of 60.0 MWt and total intrasubassembly (and intrarod) coolant flow of 8080 gpm (0.510 m^3/s) of 800°F (427°C) sodium, i.e., a discharge of about 8500 gpm

TABLE I. Calculated PRD Components (Ih) in Run 85A at 60.0 MWt.

Region	Coolant Density	Coolant Displ.	Steel Density	Bond Sodium	Fuel Axial Exp.	Doppler	B_4C-Fuel	Sums	Fraction of Total Linear Component
Core	-18.2	-4.0	-1.8	-1.3	-16.7	-2.5	0	-44.5	0.43
Above core	-17.1	-3.0	-2.4	0	0	0	+0.5	-22.0	0.22
Below core	-0.1	-0.3	-0.4	-0.0	-0.3	+0.1	0	-1.0	0.01
Rad. refl.	-4.3	-3.7	-5.4	0	0	0	—	-13.4	0.13
Rad. blkt.	-0.4	-0.3	-0.1	-0.2	-0.4	-1.5	—	-2.9	0.03
Sum	-40.1	-11.3	-10.1	-1.5	-17.4	-3.9	+0.5	-83.8	0.82
Fraction of Total Linear Component	0.39	0.11	0.10	0.01	0.17	0.04	(-0.00)	0.82	

Rod bank suspension = -19.0 (fraction = 0.18)

Linear component (including nonlinear Doppler component) = -83.8-19.0 = -102.8 (fraction = 1.00)

Linear power coeff. = $\frac{-102.8}{60.0} \equiv -1.71$ Ih/MWt

TABLE II. Calculated PRD Components (Ih) in Run 93A at 60.0 MWt.

Region	Coolant Density	Coolant Displ.	Steel Density	Bond Sodium	Fuel Axial Exp.	Doppler	B_4C-Fuel	Sums	Fraction of Total Linear Component
Core	-19.2	-4.1	-1.9	-1.2	-19.2	-3.3	0	-48.9	0.43
Above core	-18.6	-3.0	-2.4	0	0	0	+0.5	-23.5	0.21
Below core	-0.2	-0.1	-0.1	-0.0	-0.3	+0.2	0	-0.5	0.00
Rad. refl.	-5.0	-4.5	-6.7	0	0	0	—	-16.2	0.14
Rad. blkt.	-0.5	-0.3	-0.2	-0.2	-0.4	-1.7	—	-3.3	0.03
Sum	-43.5	-12.0	-11.3	-1.4	-19.9	-4.8	+0.5	-92.4	0.81
Fraction of Total Linear Component	0.38	0.11	0.10	0.01	0.17	0.04	(-0.00)	0.81	

Rod bank suspension = -21.1 (fraction = 0.19)

Linear component (including nonlinear Doppler Component) = -92.4-21.1 = -113.5 (fraction = 1.00)

Linear power coeff. = $\frac{-113.5}{60.0} \equiv -1.89$ Ih/MWt

TABLE III. Calculated PRD Components (Ih) in Run 99A at 60.0 MWt.

Region	Coolant Density	Coolant Displ.	Steel Density	Bond Sodium	Fuel Axial Exp.	Doppler	B_4C-Fuel	Sums	Fraction of Total Linear Component
Core	-18.5	-4.0	-1.6	-1.0	-18.6	-4.0	0	-47.7	0.43
Above core	-18.7	-3.3	-2.4	0	0	0	+0.5	-23.9	0.22
Below core	-0.1	-0.3	-0.4	-0.0	-0.3	+0.1	0	-1.0	0.01
Rad. refl.	-4.2	-4.5	-6.5	0	0	0	--	-15.2	0.14
Rad. blkt.	-0.5	-0.3	-0.2	-0.2	-0.4	-1.5	--	-3.1	0.03
Sum	-42.0	-12.4	-11.1	-1.2	-19.3	-5.4	+0.5	-90.9	0.83
Fraction of Total Linear Component	0.38	0.11	0.10	0.01	0.18	0.05	(-0.00)	0.83	

Rod bank suspension = -18.5 (fraction = 0.17)

Linear component (including nonlinear Doppler component) = -90.9-18.5 = -109.4 (fraction = 1.00)

Linear power coeff. = $\frac{-109.4}{60.0} \cong -1.82$ Ih/MWt

TABLE IV. Calculated PRD Components (Ih) in Run 122A at 60.0 MWt.

Region	Coolant Density	Coolant Displ.	Steel Density	Bond Sodium	Fuel Axial Exp.	Doppler	B_4C-Fuel	Sums	Fraction of Total Linear Component
Core	-21.2	-4.5	-2.0	-1.7	-15.6	-1.8	0	-46.8	0.44
Above core	-20.5	-3.5	-2.5	0	0	0	+0.6	-25.9	0.24
Below core	-0.3	-0.2	-0.2	-0.0	-0.7	+0.5	0	-0.9	0.01
Rad. refl.	-2.0	-2.1	-3.3	0	0	0	--	-7.4	0.07
Rad. blkt.	-0.2	-0.1	-0.1	-0.1	-0.3	-0.9	--	-1.7	0.02
Sum	-44.2	-10.4	-8.1	-1.8	-16.6	-2.2	+0.6	-82.7	0.78
Fraction of Total Linear Component	0.41	0.10	0.08	0.02	0.16	0.02	(-0.01)	0.78	

Rod bank suspension = -23.8 (fraction = 0.22)

Linear component (including nonlinear Doppler component) = -82.7-23.8 = -106.5 (fraction = 1.00)

Linear power coeff. = $\frac{-106.5}{60.0} \cong -1.78$ Ih/MWt

(0.536 m^3/s) from the primary pumps and a total flow through the reactor including the leakage paths of about 8190 gpm (0.517 m^3/s). The control rods are assumed to be at the 11-in. (279-mm) bank position which corresponds to the control rod fuel being displaced downward about 3.25-in. (82.6-mm) except for the high-worth Mark-II rods in which cases the fuels are displaced about 6.25 in. (159. mm). Runs 85A and 99A have one standard Mark-IA-fueled control rod and seven high-worth Mark-IA-fueled control rods. Run 93A has an additional standard Mark-IA-fueled control rod. Run 122A has instead eight Mark-II-fueled control rods, one being a standard type and seven being of the high-worth type. The listed regional core values correspond to all subassemblies through row six plus fueled subassemblies in row 7. Thus these configurations have 117, 115, 119, and 91 in-core subassemblies, respectively, for runs 85A, 93A, 99A, and 122A. The first three cases contain non-metallic fuels at some locations as well as the usual metal-fueled driver subassemblies. The corresponding number of the surrounding steel-reflector and out-of-core non-fueled subassemblies through EBR-II row 10 are then 154, 156, 152, and 180, respectively. The rows outward of row 10 for these runs contain 366 locations which are essentially all of depleted-uranium-type blanket subassemblies. Of the four cases the first three have fueled subassemblies in 27, 24, and 28 locations in row 7, respectively; whereas, run 122A has no fueled subassemblies in this row. The in-core configuration of run 122A has 76 metal-driver-fueled subassemblies (including safety rod locations), 8 metal-fueled control rod locations, and 7 in-core non-fueled locations.

The results given in Tables I to IV show that although the range of the total linear component of the PRD only varies by about 10%, individual components of the PRD for these runs can vary much more. As examples, the contribution of the steel radial reflector region varies by about 100%, the contribution of the region above core varies by about 15%, and the contribution of the rod bank suspension effect at the 11-in. (279-mm) banking varies by about 25%. Also in terms of overall-system feedback processes the steel density effect varies by about 35% and the fuel axial expansion varies by about 20%. These differences can affect modeling of calculations for comparative kinetic response studies for differing runs.

The PRD contributions of the subassemblies by fuel types and fuel-clad bond-conditions, by in-core non-fuel, by radial steel-reflector and out-of-core non-fuel, and by radial depleted-uranium-type blankets are listed in Table V for these runs. Listed are also the number of subassemblies in the various delineations given. The fueled subassemblies are listed by fuel type and bond (MF(Na), OF(He), CF(He), and CF(Na) corresponding to metal-fueled Na-bonded, mixed-oxide-fueled He-bonded, carbide-fueled He-bonded, and carbide-fueled Na-bonded, respectively) and by gap-conditions (OG, CGFF, and CGFR corresponding to open-gap, closed-gap fuel-free, and closed-gap fuel-restrained, respectively). The gap-conditions of the metal-fueled control-rod (MFR) are analogously described. The contributions listed in Table V for the control rods are for the rods at the 11-in. (279-mm) positions and assuming that the rods are not suspended from above but are supported from below at the displaced rod-bank position. The effects of rod-suspension from above are listed separately in the table.

4. NONLINEAR COMPONENTS

In Figure 2 the calculated total linear components are compared with the measured PRD values corrected to 11-in. (279-mm) bank. The deduced differences are the nonlinear components.

TABLE V. Contributions of Subassembly-types to PRDs of EBR-II Runs at 60.0 MWt

S/A Type and Gap Condition[a]	Run Number 85A No. of S/A	85A Inhours	93A No. of S/A	93A Inhours	99A No. of S/A	99A Inhours	122A No. of S/A	122A Inhours
MF(Na)OG	19	-14.4	11	-9.1	15	-10.0	18	-18.2
MF(Na)CGFF	26	-16.9	22	-15.6	29	-21.5	13	-13.7
MF(Na)CGFR	34	-19.4	39	-21.2	35	-18.4	45	-36.7
MFR(Na)OG	5	-2.5	9	-4.8	4	-1.5	2	-1.4
MFR(Na)CGFF	3	-1.3	0	0	4	-1.6	3	-1.3
MFR(Na)CGFR	0	0	0	0	0	0	3	-1.5
OF(He)OG	1	-0.8	2	-3.4	1	-1.5	0	0
OF(He)CGFF	2	-2.9	2	-2.5	1	-0.9	0	0
OF(He)CGFR	7	-4.3	12	-7.7	9	-7.1	0	0
CF(He)OG	1	-1.0	3	-3.9	2	-3.6	0	0
CF(He)CGFF	0	0	0	0	1	-0.9	0	0
CF(He)CGFR	3	-1.6	2	-1.2	4	-2.4	0	0
CF(Na)OG	2	-1.2	3	-2.6	2	-1.5	0	0
CF(Na)CGFF	0	0	0	0	0	0	0	0
CF(Na)CGFR	0	0	0	0	1	-0.5	0	0
Misc. exp.	1	-0.3	0	0	0	0	0	0
In-core non-fueled	13	-1.1	10	-0.8	11	-1.1	7	-1.0
S.S. reflectors (and out-of-core non-fueled)	154	-13.3	156	-16.2	152	-15.3	180	-7.3
Blanket (open gaps)	366	-3.0	366	-3.3	366	-3.1	366	-1.7
Rod suspension	-	-19.0	-	-21.1	-	-18.5	-	-23.8
Total	637	-103.	637	-113.	637	-109.	637	-107.

[a]MF, MFR, OF, CF, (Na or He), OG, CGFF, and CGFR refer, respectively, to metal fuel, metal-fueled control-rod, oxide fuel, carbide fuel, bond, open gap, closed-gap fuel-free, and closed-gap fuel-restrained.

It is seen that the linear components only range between about -1.7 Inhours per MWt to about -1.9 Inhours per MWt for these runs; whereas, the deduced non-linear components vary greatly. Thus run 85A exhibits a strongly negative non-linear PRD component, run 93A exhibits a strongly positive non-linear PRD component, run 99A exhibits very little non-linear component, and run 122A exhibits a negative non-linear component at lower powers and a positive non-linear component at the higher powers.

It is anticipated that such analyses of the linear components will give improved confidence in the deduction of the non-linear components so as to enable the sub-assembly-bowing phenomena primarily responsible for the non-linear components to be better understood.

5. DIFFERING GAP-CONDITIONS

The calculations of the linear (and Doppler) components of the PRD for run 93A have been also carried out assuming idealizations of all fuel-to-clad gaps having

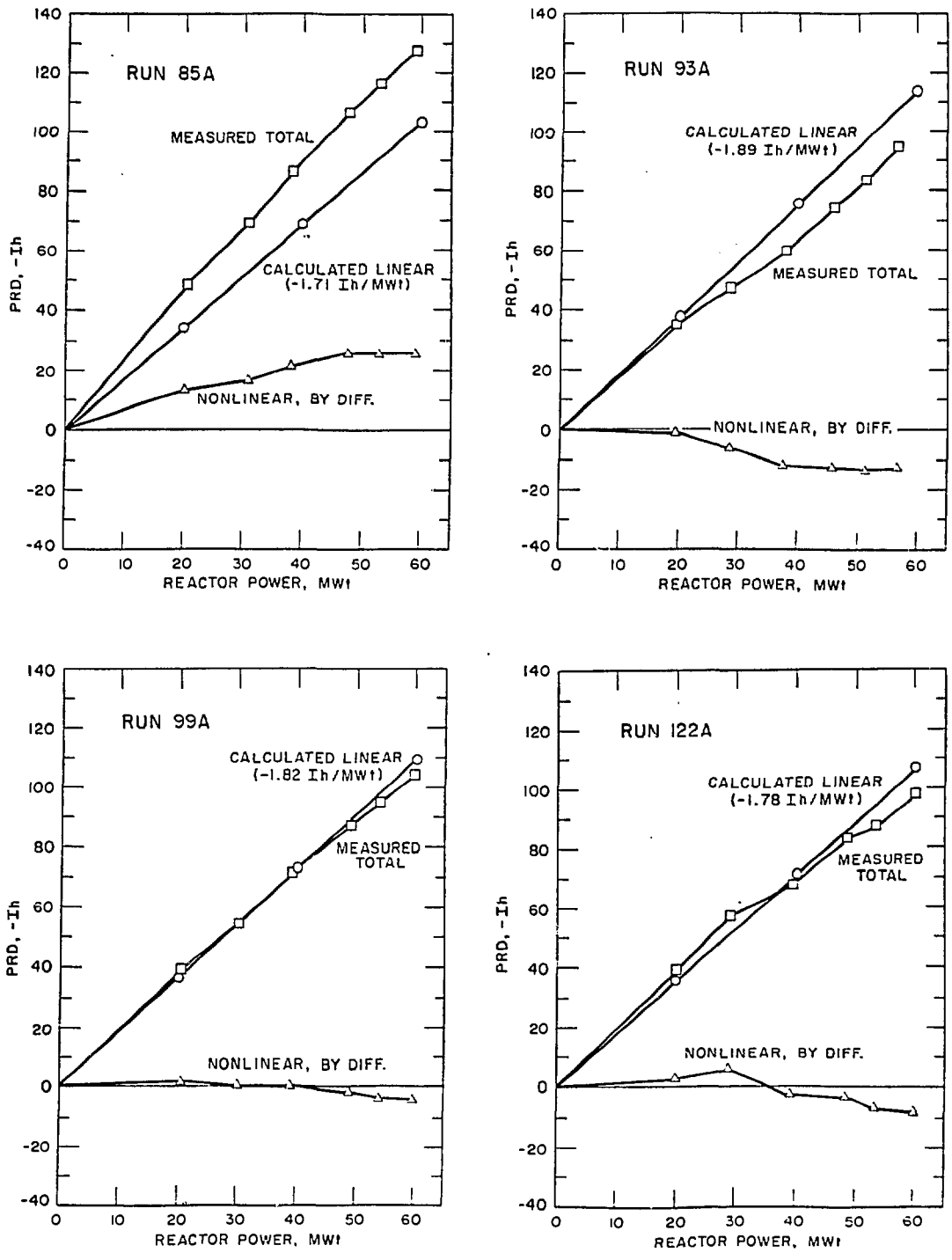

Figure 2. Calculated Total Linear PRD Components and Measured Total PRD Values for EBR-II Runs 85A, 93A, 99A, and 122A.

identical conditions simultaneously i.e., gaps all open, gaps all closed but not restrained axially by the cladding circumference, and gaps all closed but axially restrained by the fuel-to-clad binding (fuel expands axially with the expansion of the cladding). For the latter two conditions in the case of the Mark-II fuel the assumption of no sodium as well as that of sodium in about one-third of the fuel porosities were considered. These results are given in Table VI.

TABLE VI. Effects of Differing Gap-conditions on PRD *Components for Run 93A at 60.0 MWt*

No. of S/A	Type[a]	Gap Condition: Open-gaps (OG)	Closed-gaps Fuel-free (CGFF)	Closed-gaps Fuel-restrained (CGFR)	93A Distribution
72	MF(Na)	-52.7 Ih	-50.3[b] Ih	-41.6[c] Ih	-46.0 Ih
9	MFR(Na)	-4.8	-4.5	-4.5	-4.8
16	OF(He)	-21.1	-18.0	-11.6	-13.7
5	CF(He)	-7.1	-4.8	-2.9	-5.1
3	CF(Na)	-2.6	-2.7	-1.8	-2.6
366	Blkts. (Na)	-3.3	-3.2	-3.1	-3.3
10	In-core Non-fuel	-0.8	-0.8	-0.8	-0.8
156	S.S. Refl.	-16.2	-16.2	-16.2	-16.2
Rod Suspensions		-21.1	-21.1	-21.1	-21.1
Sums		-129.7 Ih	-121.6 Ih	-103.6 Ih	-113.6 Ih
Linear Power Coeff.		-2.16 Ih/MWt	-2.03 Ih/MWt	-1.73 Ih/MWt	-1.89 Ih/MWt

[a]MF, MFR, OF, CF and (Na or He), refer, respectively, to metal fuel, metal-fueled control-rod, oxide fuel, carbide fuel, and bond.

[b]Assuming no sodium in Mark-II fuel porosities; -47.6 Ih assuming sodium in about one-third of interconnected porosities of Mark-II fuel.

[c]Assuming sodium in about one-third of interconnected porosities of Mark-II fuel; -41.7 Ih assuming no sodium in Mark-II fuel porosities.

The linear power coefficient values range from -2.16 Ih/MWt for all fuels simultaneously having completely open gaps to -1.73 Ih/MWt for all fuels having completely closed gaps with all fuels limited in axial expansions by the axial expansions of the claddings. The values for these extreme gap-conditions may be compared with the value -1.89 Ih/MWt obtained using the distributions of the gap-conditions assumed in the analysis of run 93A.

The corresponding ranges of the contributions to the PRD per subassembly at 60.0 MWt for the fuel types are: -0.73 Ih/sa to -0.58 Ih/sa (about 20%) for the average of the 72 metal-fueled subassemblies; -1.32 Ih/sa to -0.73 Ih/sa (about 45%) for the average of the 16 oxide-fueled subassemblies; -1.42 Ih/sa to -0.58 Ih/sa (about 60%) for the average of the 5 carbide-fueled helium-bonded subassemblies; and -0.87 Ih/sa to -0.60 Ih/sa (about 30%) for the average of the 3

carbide-fueled sodium-bonded subassemblies. These results show the sensitivities of the PRD to fuel types and to gap conditions and enable estimates of the importance of these considerations in the PRD interpretations of EBR-II loadings to be made.

6. DIFFERING ROD-BANK POSITIONS

In the analyses described in the above sections, the control-rod-bank was assumed to be at the 11-in. position. Results of analyses of the effects of other assumed rod-bank positions upon the linear component of the PRD for run 93A are given here.

As stated above, in run 93A there were two standard Mark-IA control rods and seven high-worth Mark-IA control rods. At the fully up 14-in. (356-mm) position, the bottom of the fuel in these rods is about 0.25 in. (6.4 mm) below the bottom of the core fuel. At the 11-in. (279-mm) position, the bottom of the rod fuel is about 3.25 in. (82.6 mm) below the core. At the 6-in. (152-mm) position and the 2-in. (51-mm) position, the bottom of the rod fuel is about 8.25 in. (210 mm) and 12.25 in. (311 mm), respectively, below the core.

The calculational estimates of the rod-bank effects were made in two steps. First, the linear PRDs with the rods at various bank positions were calculated assuming the rod not suspended from above but supported from below at the displaced rod-bank position. Then the PRD effects upon these displaced rods resulting only from their suspension from above (instead of support from below) were estimated. Table VII lists the linear power-coefficient components contributed by these two assumptions for the rods at the 14-in., 11-in., 6-in., and 2-in. positions. It is seen that the change in bank position with supported rods varies the power coefficient by only a few percent, because the nine rods contain only a small fraction of the fuel in the reactor. The coefficients with suspended rods, however, vary considerably because of the combination of the effective rod-suspension shaft lengths and the differential worths of the rods at the various positions.

TABLE VII. Linear Power Coefficients, Ih/MWt

Rod Bank, in.	Total with Supported Rods	Addition Due to Rod Suspension	Total
14	-1.55	-0.16	-1.71
11	-1.54	-0.35	-1.89
6	-1.50	-0.59	-2.09
2	-1.52	-0.51	-2.03

7. CONCLUSIONS

Comparisons of corresponding components of the PRDs of these four EBR-II configurations show that many of the components differ substantially. In particular the contribution of the radial steel-reflector can vary greatly depending upon core size.

The effects of differing extreme-assumptions upon fuel-clad gap conditions range from about 20% for metal-fueled subassemblies to about 60% for oxide-fueled subassemblies.

The rod-bank suspension contribution is dependent on banking positions of the control rods and on the complement of control-rod types, as well as the loading configuration of the run.

These results show the importance of detailed analyses to obtain the linear components of the PRDs of EBR-II configurations and to enable the non-linear components to be more confidently deduced by comparisons with PRD measurements. Effects of components exhibiting significant ranges should be considered in kinetics analyses because components can have differing time-dependencies.

REFERENCES

[1] D. Meneghetti and W. B. Loewenstein, "EBR-II Irradiation Physics," National Topical Meeting on New Developments in Reactor Physics and Shielding, CONF-72091 Book 2 (1972), p. 905.

[2] D. Meneghetti and D. A. Kucera, "EBRPOCO-A Program to Calculate Detailed Contributions of Power Reactivity Components of EBR-II," Proc. Int. Topical Meeting on Advances in Mathematical Methods for the Solution of Nuclear Engineering Problems, Vol. 2, Munich, (1981) p. 225.

[3] F. R. Mynatt, DOT, A Two-Dimensional Discrete Ordinate Code, K-1694, Radiation Shielding Information Center, Oak Ridge National Laboratory (1967).

[4] T. B. Fowler, D. R. Vondy, and R. W. Cunningham, Nuclear Reactor Core Analyses Code: CITATION, ORNL-RM-2496, Revision 2 (1971).

[5] A. Gopalakrishnan and J. L. Gillette, "EBRFLOW-A Computer Program for Predicting the Coolant Flow Distribution in the Experimental Breeder Reactor-II," Nuclear Technology, 17, 3, (1973) p. 205.